Identification of *cis*-Ethanesemidione as the Organic Radical Derived from Glycolaldehyde in the Suicide Inactivation of Dioldehydrase and of Ethanolamine Ammonia-Lyase†

Andreas Abend,‡ Vahe Bandarian,§ George H. Reed,* and Perry A. Frey*

Institute for Enzyme Research, The Graduate School, and Department of Biochemistry, College of Agricultural and Life Sciences, University of Wisconsin−Madison, Madison, Wisconsin 53705

Received December 27, 1999; Revised Manuscript Received March 7, 2000

ABSTRACT: The hydrate of glycolaldehyde is a substrate analogue that induces the formation of cob(II)alamin and 5′-deoxyadenosine from adenosylcobalamin at the active site of dioldehydrase, and the resulting complex is inactive. The carbon atoms of glycolaldehyde hydrate remain bound to this complex, and it has been postulated that the first step or steps of the catalytic process on glycolaldehyde hydrate generate an intermediate that undergoes a destructive side reaction leading to inactivation of the enzyme [Wagner, O. W., Lee, H. A., Jr., Frey, P. A., and Abeles, R. H. (1966) *J. Biol. Chem. 249*, 1751−1762]. All evidence suggests that dioldehydrase reaction proceeds by a radical mechanism, and the glycolaldehyde hydrate is expected to be converted initially into a radical. Electron paramagnetic resonance (EPR) spectroscopic analysis of the inactivated complex shows that glycolaldehyde is transformed into a *cis*-ethanesemidione radical that is weakly spin-coupled to the cob(II)alamin in the active site of the enzyme. This radical has been identified by analysis of EPR spectra obtained from samples with ^{13}C- and ^{2}H-labeled forms of glycolaldehyde. The analysis shows that the stable radical associated with the inactive complex is symmetrical and that it contains a single solvent-exchangeable proton, consistent with a *cis*-ethanesemidione. Glycolaldehyde also inactivates ethanolamine ammonia-lyase (EAL). EPR studies of ethanolamine ammonia-lyase reveal that treatment with glycolaldehyde also results in formation of an ethanesemidione radical bound in the active site. The suicide inactivation in both enzymatic reactions is postulated to result from formation of this stable radical, which cannot react further to abstract a hydrogen atom from 5′-deoxyadenosine. Analysis of the electron spin−spin coupling between the semidione radicals and cob(II)alamin in both enzymes indicates that the distance between the radical and Co^{2+} is ∼11 Å in each case.

Coenzyme B_{12}-dependent dioldehydrase (DDH,[1] E.C. 4.2.1.28) catalyzes the dehydration of short-chain, vicinal diols to the corresponding aldehydes (*1*). Coenzyme B_{12} is postulated to function as a radical initiator in enzymatic reactions (*2*−*4*). Available evidence indicates that the function of coenzyme B_{12} in enzymatic rearrangements, as currently conceptualized, is as outlined in Scheme 1. This scheme accounts for the fact that hydrogen transfer by the coenzyme is mediated by carbon 5′ of the adenosyl moiety. The weakness of the cobalt−carbon bond (*5*, *6*) makes it subject to homolytic cleavage when the substrate binds to the active site. The cleaved state is thought to include B_{12r} and the 5′-deoxyadenosyl radical, a highly reactive species that can abstract an unactivated hydrogen atom from a substrate to form 5′-deoxyadenosine and a substrate radical. The substrate radical undergoes isomerization to the product-related radical, and abstraction of a hydrogen atom from 5′-deoxyadenosine by the product radical completes the reaction and allows coenzyme B_{12} to be regenerated by recombination of B_{12r} with the 5′-deoxyadenosyl radical. In coenzyme B_{12}-dependent ribonucleotide reductase, the coenzyme also functions as a radical initiator, but the radical that it generates is a thiyl radical from a cysteinyl side chain. The thiyl radical mediates the reduction of ribonucleotides to deoxyribonucleotides (*4*, *7*, *8*).

The substrate radical implied by Scheme 1 for the reaction of DDH is shown in Scheme 2, which outlines the supposed course of product formation without specifying the details

† This research was supported by NIH Grants GM35752 (G.H.R.), DK28607 (P.A.F.), and a postdoctoral fellowship (A.A.) from the Deutsche Forschungsgemeinschaft. This study made use of the National Magnetic Resonance Facility at Madison, which is supported by NIH Grant RR02301 from the Biomedical Research Technology Program, National Center for Research Resources. Equipment in the facility was purchased with funds from the University of Wisconsin, the NSF Biological Instrumentation Program (DMB-8415048), NSF Academic Research Instrumentation Program (BIR-9214394), NIH Biomedical Research Technology Program (RR02301), NIH Shared Instrumentation Program (RR02781 and RR08438), and the U.S. Department of Agriculture.

* Address correspondence to this author at the Institute for Enzyme Research, University of Wisconsin, 1710 University Ave., Madison, WI 53705. Telephone (608) 262-0055; FAX (608) 265-2904.

‡ Present address: Merck & Company, Inc., Sumneytown Pike, P.O. Box 4, West Point, PA 19486-0004.

§ Present address: Biophysics Research Division, University of Michigan, Chemical Sciences Bldg., 930 N. University Ave., Ann Arbor, MI 48109-1055.

[1] Abbreviations: DDH, dioldehydrase; EAL, ethanolamine ammonia-lyase; DTT, dithiothreitol; coenzyme B_{12}, adenosylcobalamin; B_{12r}, cob(II)alamin; HPLC, high-performance liquid chromatography; EPR, electron paramagnetic resonance; NMR, nuclear magnetic resonance; Hepes, *N*-(2-hydroxyethyl)piperazine-*N*′-2-ethanesulfonic acid.

10.1021/bi992963k CCC: $19.00
Published on Web 04/27/2000

Scheme 1

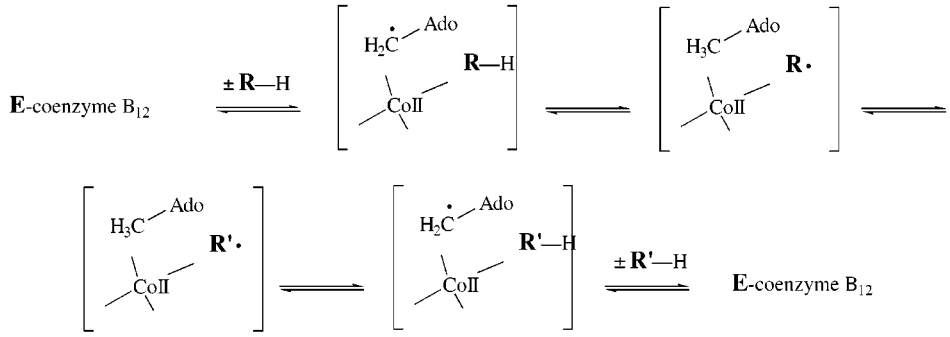

Scheme 2

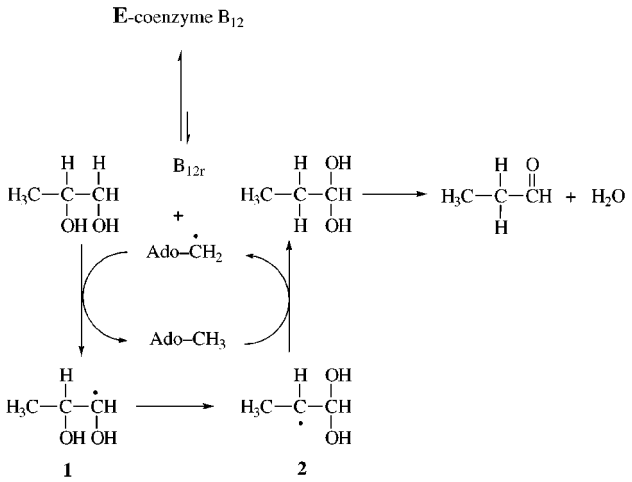

of the radical rearrangement mechanism. The isomerization of 1,2-propanediol at the active site leads to propionaldehyde hydrate, which is enzymatically dehydrated to propionaldehyde (*9*). The stereochemistry of the reaction of 1,2-propanediol is interesting, in that both (*R*)- and (*S*)-propanediol are substrates and one or the other hydrogen atom is abstracted from C1 depending on the configuration at C2 (*10*). The structures of the intermediates shown in Scheme 2 remain hypothetical; however, spectroscopic evidence for radical intermediates has been published (*11*, *12*). Recently, a high-resolution structure of DDH has been published (*13*).

In early studies of the mechanism of action of DDH, Abeles and co-workers observed its suicide inactivation by glycolaldehyde, a structural analogue of 1,2-propanediol or ethylene glycol (*14*). Glycolaldehyde inactivates the complex of DDH with coenzyme B_{12} within a few seconds. Inactivation is accompanied by the formation of a new complex of DDH, which includes B_{12r} and 5′-deoxyadenosine in place of coenzyme B_{12}. The carbon atoms of glycolaldehyde remain tightly bound to this complex, and upon its denaturation by acidification in the air, the product derived from glycolaldehyde is glyoxal. This early study demonstrated the presence of B_{12r} and 5′-deoxyadenosine in a coenzyme B_{12}-dependent reaction. However, the structure of the enzyme-bound product derived from glycolaldehyde was not elucidated. In the present paper, EPR spectroscopy and isotopically labeled forms of glycolaldehyde are used to characterize the radical species derived from glycolaldehyde in the inactivation of DDH and the related enzyme EAL. The weak magnetic interactions between the radicals and the low-spin Co^{2+} of B_{12r} were used to determine the separation of the two paramagnetic species in the respective active sites.

EXPERIMENTAL PROCEDURES

Materials. [1,3-$^{13}C_2$]glycerol, [2-^{13}C]glycerol, and [$^2H_5$]-glycerol were from Isotec. ^2H_2O, ammonium bicarbonate, *p*-nitrophenyl hydrazine and $NaIO_4$ were from Aldrich. Coenzyme B_{12}, NADH, ATP, and glycolaldehyde were from Sigma. Centricon 30 was from Amicon. The genes coding for the α, β, and γ subunits of DDH of *Salmonella typhimurium* (*15*) were expressed in *Escherichia coli*, and the apoprotein (specific activity 95 IU mg^{-1}) was purified as described previously (*16*). Recombinant EAL from *S. typhimurium* (*17*) was expressed in *E. coli*. The protein (specific activity 45 IU mg^{-1}) was isolated as described previously (*18*). Glycerol kinase, glycerol-3-phosphate dehydrogenase, acid phosphatase, and alcohol dehydrogenase were from Boehringer Mannheim. Samples containing coenzyme B_{12} were handled under dim light to prevent photolysis. No steps were taken to exclude O_2 from the samples.

Analytical Methods. Aldehydes, separated from reaction mixtures, were spotted on a silica gel plate, dried with a heating gun, and stained with *p*-nitrophenyl hydrazine to form the corresponding yellow-orange hydrazones. Glycerol 3-phosphate and glycolaldehyde were determined enzymatically with glycerol-3-phosphate dehydrogenase and alcohol dehydrogenase, respectively.

Chromatographic Systems. Glycerol 3-phosphate and glycolaldehyde phosphate were purified from the corresponding reaction mixtures on a column of DEAE-Sephadex A-25 (Pharmacia, 30 cm × 2.6 cm) equilibrated in 10 mM ammonium bicarbonate and eluted by applying a linear gradient of ammonium bicarbonate increasing from 10 to 400 mM in a total volume of 2 L. The flow rate was adjusted to 2 mL min^{-1}, and 20 mL fractions were collected. Solutions of glycolaldehyde were deionized by passage over a mixed-bed resin prepared from DEAE-Sephadex A-25 (OH^- form) and SP-C25-Sephadex (H^+ form, Pharmacia). Analytical HPLC was performed on a Waters system with an anion-exchange column (Vydac, 25 cm × 4.6 cm, equilibrated in 50 mM KH_2PO_4, pH 4.2) eluted with a gradient from 10% buffer B (1 M NaCl in 50 mM KH_2PO_4, pH 4.2) to 90% B in 12 min (flow rate 1.5 mL min^{-1}, detection at 254 nm).

Spectroscopy. ^{1}H and ^{31}P NMR data were recorded on a Bruker WP200 spectrometer, and ^{13}C NMR data were recorded on a Bruker DMX 500. EPR spectra were recorded at X-band (∼ 9.1 GHz) with a Varian E-3 spectrometer.

Samples were maintained at 77 K using a standard liquid nitrogen immersion Dewar.

Synthesis of Isotopically Labeled Glycerol-3-phosphates. [1,3-$^{13}C_2$]Glycerol (250 mg, 2.7 mmol) was phosphorylated enzymatically to L-(−)-[1,3-$^{13}C_2$]glycerol 3-phosphate by use of 100 units of glycerol kinase and 3 mmol of MgATP at 27 °C. The reaction was carried out in a total volume of 30 mL of 100 mM glycine buffer containing 40 mM $MgSO_4$, 2 mM DTT, and 1 mM EDTA at pH 9.5. The progress of the reaction, which was complete after 4 h, was monitored by following the conversion of ATP to ADP by analytical anion exchange chromatography. The reaction mixture was diluted with water to a final volume of 0.2 L, charged on a column of DEAE-Sephadex A-25 (2.5 × 30 cm) and separated under the above-described conditions. Fractions containing L-(−)-[1,3-$^{13}C_2$]glycerol 3-phosphate were detected enzymatically by the use of glycerol-3-phosphate dehydrogenase to measure NADH formation spectrophotometrically at 340 nm. The compound emerged in 90% yield at 0.2 M ammonium bicarbonate. Fractions containing the product were evaporated to dryness. The syntheses of [2-^{13}C]glycerol-3-phosphate and [$^2H_5$]glycerol-3-phosphate were similar, starting from the corresponding isotopically labeled glycerol, to that described in detail for [1,3-$^{13}C_2$]glycerol-3-phosphate.

Synthesis of [1-^{13}C]Glycolaldehyde Phosphate, [2-^{13}C]Glycolaldehyde phosphate, [$^2H_3$]Glycolaldehyde phosphate, and [1-^{2}H]Glycolaldehyde. Each labeled glycerol 3-phosphate (1 mmol) was dissolved in 10 mL of water. An aliquot (10 mL) of 200 mM $NaIO_4$ was added to each solution, which was shaken occasionally. After 20 min, the reaction was quenched by addition of 6 mmol of ethylene glycol. Each solution was diluted to 0.1 L with water and loaded on individual columns of DEAE-Sephadex A-25. The chromatographic conditions were the same as for glycerol 3-phosphate. An aliquot (5 μL) of each fraction was spotted on a silica plate, and the aldehyde was detected as its *p*-nitrophenyl hydrazone by dipping the plates into an acidic solution containing *p*-nitrophenyl hydrazine [5% in ethanol/H_2SO_4 (95:5)] and evaporating the solvent with a heat gun. The compound emerged from the column in 70% yield at 0.25 M ammonium bicarbonate.

Synthesis of [1-^{13}C]Glycolaldehyde, [2-^{13}C]Glycolaldehyde, and [$^2H_3$]Glycolaldehyde. The individual glycolaldehyde phosphates (0.5 mmol) were dephosphorylated enzymatically by acid phosphatase at 30 °C in total volume of 2 mL (100 units in 300 mM citric acid, pH 6.0, and 5 mM DTT). The progress of the reaction was monitored by ^{31}P NMR, which showed complete removal of the phosphate group from the aldehyde after 30 min. The solution was passed over a mixed-bed resin column (1 × 7.5 cm) and washed with water. Fractions were checked enzymatically for glycolaldehyde by the use of alcohol dehydrogenase and NADH. The water was removed from the product by evaporation, and the compound was obtained in 95% yield and stored at −20 °C.

Preparation of Glycolaldehyde-Inactivated DDH for EPR Analysis. DDH (200 μL), 400 mM (active sites), in buffer A (50 mM potassium phosphate, pH 8.0, 125 mM 1,2-propanediol, and 23 mM sodium cholate) was incubated with 20 μL of coenzyme B_{12} (2 mM) for 5 min at 37 °C in the dark. Glycolaldehyde (10 μL, 5 mM), in unlabeled or ^{2}H- or ^{13}C-labeled form, was added to the holoenzyme. Following incubation for 2 min at 37 °C in the dark, the samples were frozen in liquid nitrogen. Samples of DDH in ^2H_2O were prepared by diluting 1 mL of enzyme (400 μM active sites) into 10 mL of buffer A made up in ^2H_2O (pD 8.0) and subsequent concentration on Centricon 30. This step was repeated twice and the final ratio of protium to deuterium in the solvent was <1%. To obtain protein samples with different ^2H_2O content, the sample in ^2H_2O was added to appropriate amounts of an equally concentrated DDH sample in H_2O (aqueous buffer A). Coenzyme B_{12} and glycolaldehyde samples in various $^2H_2O/H_2O$ mixtures were prepared in the same manner.

Inactivation of EAL by Glycolaldehyde. A solution of EAL and coenzyme B_{12} (3 μM) in 10 mM Hepes-NaOH, pH 7.5) was exposed to 10 mM glycolaldehyde and aliquots were diluted at various times and assayed with ethanolamine as the substrate by the coupled assay with alcohol dehydrogenase and NADH. A control sample without glycolaldehyde was assayed in parallel.

Preparation of Glycolaldehyde-Treated EAL for EPR Analysis. The samples (250 μL) were prepared by mixing EAL (200 μL, ∼0.2 mM active sites, 10 mM Hepes-NaOH, pH 7.5) with 50 μL of a solution of coenzyme B_{12} (2 mM) and glycolaldehyde or isotopically labeled glycolaldehyde (1.6 mM). The samples were transferred to EPR tubes and frozen within 1 min of mixing.

Interpretation of EPR Spectra. The radicals that are generated from glycolaldehyde in the active sites of DDH and EAL are magnetically coupled to the unpaired electron spin of the low-spin Co^{2+} of B_{12r}, which is also generated in the reaction. The coupling between the two paramagnetic centers alters the appearance of the EPR spectra of the spin-coupled partners. EPR spectra were interpreted by use of a spin Hamiltonian (eq 1) which includes an isotropic exchange coupling, *J*, and a through-space dipole−dipole coupling tensor, **D**:

$$H_s = \beta\vec{H}\cdot\mathbf{g}_1\cdot\vec{S}_1 + \beta\vec{H}\cdot\mathbf{g}_2\cdot\vec{S}_2 + J\vec{S}_1\cdot\vec{S}_2 + \vec{S}_1\cdot\mathbf{D}\cdot\vec{S}_2 \qquad (1)$$

In eq 1, $\vec{H}$ is the laboratory magnetic field and $\mathbf{g_1}$ and $\mathbf{g_2}$ are the *g* tensors of the low-spin Co^{2+} and radical, respectively. Simulations were performed for perdeuterated samples, and the nuclear hyperfine coupling terms normally included in eq 1 were not required in the simulations. Field-swept powder-pattern EPR spectra were simulated by diagonalization of the energy matrix derived from eq 1 as described previously (*18*).

RESULTS AND DISCUSSION

Observation of a Radical in Glycolaldehyde-Inactivated DDH. Samples of DDH holoenzyme were prepared by incubation of the enzyme with coenzyme B_{12}. Addition of glycolaldehyde led to inactivation and conversion of coenzyme B_{12} into B_{12r}, as originally observed spectrophotometrically (*14*) and verified by EPR spectroscopy (*16*). EPR spectra of the freshly prepared samples (Figure 1) show an altered spectrum due to B_{12r} and a relatively narrow signal centered about *g* 2.0 from another paramagnetic species. The position and width of the second species were consistent with those of an organic radical. Because the nucleoside product of the inactivation reaction had been shown to be 5′-

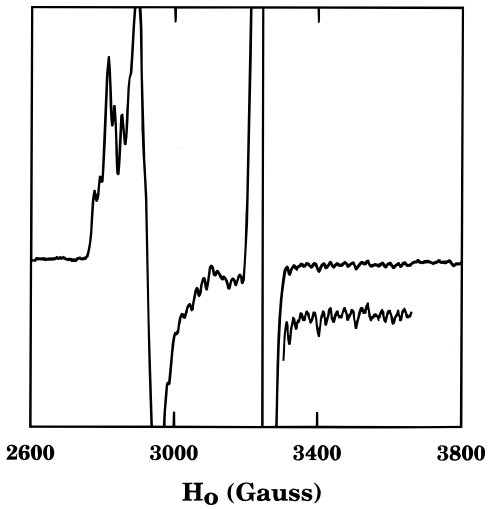

FIGURE 1: X-band EPR spectrum of a sample of DDH-coenzyme B_{12} following inactivation by glycoaldehyde, showing an altered pattern for the low-spin Co^{2+} and a signal from an organic radical. Signals from the $g_{\perp}$ region of the Co^{2+} spectrum and signals of the radical are off scale in order to highlight the altered ^{59}Co hyperfine signals in the $g_{||}$ region. The quintet patterns for the ^{59}Co hyperfine transitions in the $g_{||}$ region (shown at 3× gain in the inset trace) are explained in the caption for Figure 4. The spectrum was obtained at 77 K at a microwave frequency of 9.09 GHz and 16 mW microwave power. The composition of the sample is given under Experimental Procedures.

deoxyadenosine (*14*), attention was focused on a product derived from glycolaldehyde as a candidate for the putative radical.

Location of the Unpaired Spin Density. To identify the organic radical, inactivation mixtures were prepared with isotopically labeled glycolaldehyde. Spectra from samples prepared with either [1-^{13}C]glycolaldehyde or [2-^{13}C]glycoaldehyde are indistinguishable (Figure 2, spectra B and C, respectively), and both are slightly broader than those of unlabeled samples (Figure 2A). Incubation of holo-DDH with deuterated glycolaldehyde led to collapse of the features within the envelope of the spectrum, as shown in Figure 2D. These data unambiguously place the unpaired spin density on the product derived from glycolaldehyde.

Solvent-Exchangeable Site of the Radical. Incubation of holo-DDH with deuterated glycolaldehyde in ^2H_2O narrows the spectrum (Figure 2E), indicating the presence of at least one solvent-exchangeable proton within the radical. The spectrum of a sample prepared in a mixture of H_2O/D_2O (50:50) could be reproduced by the summation of equal amounts of the spectra obtained in 100% H_2O and in 100% D_2O (Figure 3). This result indicates that there is a single,[2] solvent-exchangeable proton present in the radical.

Structure of the Radical. The changes observed in the spectra upon introduction of ^{13}C into the glycolaldehyde backbone are modest and not consistent with those expected of a carbon-centered radical, which would typically exhibit an axial ^{13}C hyperfine splitting tensor with the largest component ($A_z \sim 70$ G) parallel to the half-filled p orbital (*19*). Small ^{13}C hyperfine splitting constants ($a_C \leq 5$ G) have, however, been observed in semidione radicals in solution

[2] For example, based on two solvent-exchangeable sites, the statistical weights of the signals corresponding to $^1H_2$, $^2H_2$, $^1H/^2H$, and $^2H/^1H$ species are each 25%.

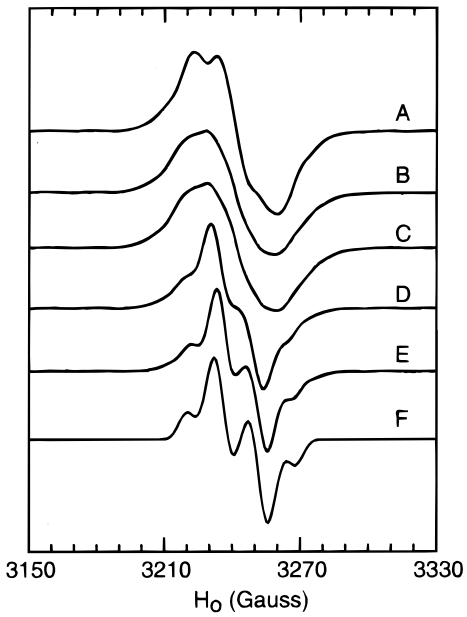

FIGURE 2: EPR spectra of the radical region of samples of DDH-coenzyme B_{12} after inactivation by glycoaldehyde and isotopically substituted forms of glycoaldehyde. (A) Unlabeled glycoaldehyde in water; (B) [C1-^{13}C]glycoaldehyde in water; (C) [C2-^{13}C]glycoaldehyde in water; (D) [$^2H_3$]glycoaldehyde in water; (E) [$^2H_3$]glycoaldehyde in ^2H_2O; (F) simulation of the pattern in spectrum E with $D = -22$ G and $J = -3$ G. Spectra were obtained at 4 mW microwave power at 77 K.

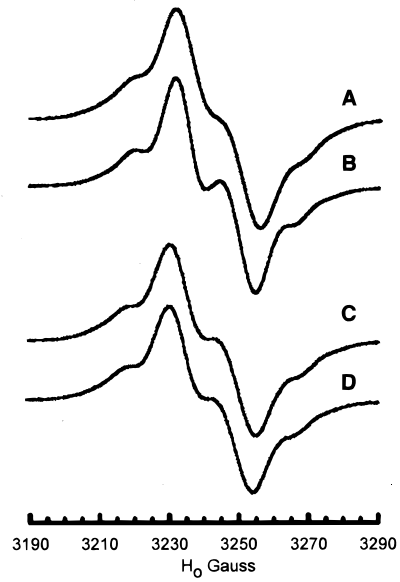

FIGURE 3: EPR spectra of the radical region of samples of DDH-coenzyme B_{12} inactivated with [$^2H_3$]glycoaldehyde in H_2O (A), in 99.9% ^2H_2O (B), and in 50% ^2H_2O (C). Spectrum D was obtained by addition of equal amounts of signals A and B.

(*20*). Semidiones are planar radicals wherein the unpaired electron is contained within a π-molecular orbital that is made up from p orbitals of both oxygen and both carbon atoms of the radical. Experimental observations on semidione radicals indicate that the unpaired spin density is approximately equally distributed among the four atoms of the semidione backbone. Hyperfine splittings, $a_H = 7.7$ G, from the protons in the ionized version of the ethanesemidione radical, the glyoxal radical anion (*20*), are consistent with the present observation of a significant narrowing of the signals for samples prepared with perdeuterio glycolaldehyde.

Chart 1

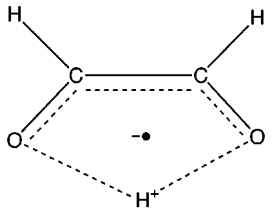

All of the changes in the EPR signals upon isotopic substitutions in glycolaldehyde and in the solvent are therefore consistent with those expected of a neutral *cis*-ethanesemidione radical (or the neutral radical of glyoxal), the structure of which may be represented as in Chart 1.

Electron Spin−Spin Interactions. The EPR spectrum of the radical responds to isotopic substitutions in the parent glycolaldehyde in a manner expected of a *cis*-ethanesemidione radical. The overall shape of the spectral envelope and the symmetrical pattern that remains in the spectra of samples prepared with perdeuterio glycolaldehyde (Figure 2D,E), however, reflect the magnetic interaction of the electron spin of the radical with that of the unpaired electron in the d_z^2 orbital of the Co^{2+} of the B_{12r} with which the radical shares the active site. The nearly symmetrical, four-line pattern (Figure 2D,E) is reminiscent of a classical "Pake doublet" wherein the outer lines are separated by 2*D* and the inner lines are separated by *D*, where *D* is the dipole−dipole interaction parameter (*21*). The pattern observed for the semidione radical varies slightly from that expected for a Pake doublet arising from purely dipolar interactions because of a small contribution from an isotropic exchange interaction. The classical Pake line shape is modified by an exchange interaction such that the separation of the inner lines becomes $|J - D|$ and that of the outer lines is $|J + 2D|$ (*18*). For dipole−dipole coupling, *D* carries a negative sign (*22*), and for the sign convention used in eq 1, a positive *J* corresponds to an antiferromagnetic exchange interaction. Simulation of the pattern indicates that $D \sim -21$ G and $J \sim -3$ G (Figure 2F). The *g* anisotropy of the Co^{2+} contributes slightly to the measured exchange coupling ($J_d \sim -1.6$ G) (*23*). The sign of *J* that emerges from the analysis indicates a very weak ferromagnetic exchange coupling between the two paramagnetic centers.

The EPR signals of the low-spin Co^{2+} are also altered by the electron spin−spin coupling with the semidione radical (Figure 1). When bound to DDH, in isolation from other paramagnetic species, the Co^{2+} of B_{12r} yields an EPR spectrum with an axially symmetric *g* tensor and a ^{59}Co hyperfine tensor of axial symmetry (*16*). Hyperfine coupling with the nuclear spin of ^{59}Co ($I = {}^7/_2$) results in a resolved ($A_{||} \sim 110$ G) octet of signals centered about $g_{||} \sim 2.01$. These ^{59}Co hyperfine signals are split into triplets through superhyperfine coupling to the ^{14}N ($I = 1$) of the axial dimethylbenzimidazole ligand ($A_{14N} \sim 21$ G) (*13*, *16*, *24*). In the spectrum of the spin-coupled pair (Figure 1) the ^{59}Co hyperfine transitions of B_{12r} in the region of $g_{||}$ appear as sets of five line patterns with intensities of 1:1:2:1:1. These five-line patterns are composed of an overlapping doublet of triplets as shown in Figure 4. The doublet splitting is from the electron spin−spin interaction, which is $|J + 2D|$ in the parallel orientation. The magnitude of $|J + 2D|$ is coincidentally approximately twice the superhyperfine splitting

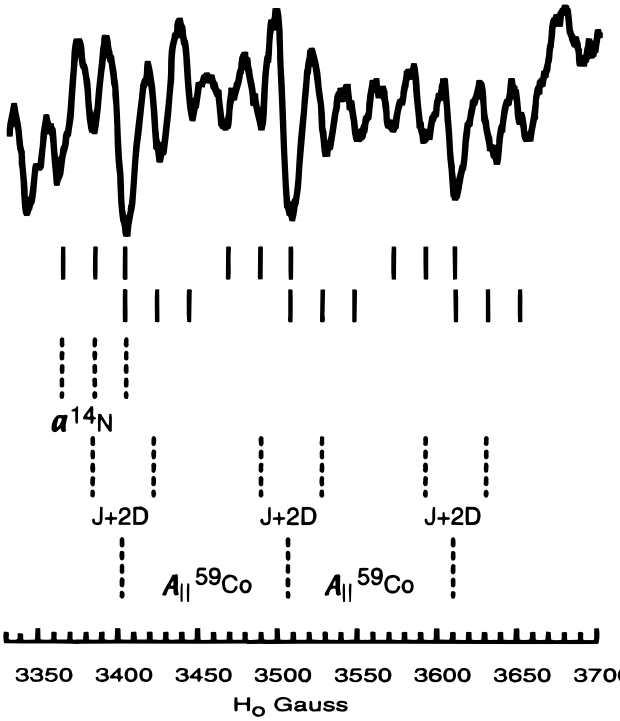

FIGURE 4: EPR spectrum of DDH-coenzyme B_{12} following inactivation by glycoaldehyde, showing three of the eight ^{59}Co hyperfine transitions in the $g_{||}$ region. As indicated in the figure, the hyperfine splitting is $A_{||}$ ^{59}Co. An electron spin−spin splitting $= |J + 2D|$ creates an overlapping doublet of triplets from the superhyperfine splitting of ^{14}N of the dimethylbenzimidazole ligand of the Co^{2+}. In this case $|J + 2D| \approx 2a^{14}N$, which explains the 1:1:2:1:1 intensity pattern.

from the ^{14}N, and this circumstance accounts for the multiplicity and intensity of the five-line pattern. The value of $|J + 2D|$ obtained from splitting of the signals of Co^{2+} agrees with the value obtained from simulation of the powder pattern from the radical. The observation that the maximum dipole−dipole splitting occurs in the $g_{||}$ region of the Co^{2+} spectrum indicates that the radical to Co^{2+} interspin vector lies approximately along the axis of the d_{z^2} orbital of the Co^{2+}. This finding is compatible with the crystal structure, which shows that 1,2-propanediol binds directly above Co^{2+} in the active site (*13*). Even in the absence of electron spin−spin coupling, the $g_\perp$ region of the spectrum of low-spin Co^{2+} in B_{12r} is complicated (*25*). The electron spin spin coupling in the present case creates an additional splitting of the existing signals by $|J - D|$.

Radical to Co^{2+} Distance Estimate. The effects of the electron spin−spin interactions on the EPR signal of the radical and of the low-spin Co^{2+} permit a fairly accurate determination of the magnitude of the dipole−dipole interaction, *D*. Moreover the modest magnitude of the dipole−dipole interaction ($D \sim -21$ G) and the small contribution from exchange validate use of the point dipole approximation (*26*) for distance estimates (in angstrom):

$$R = [(6.95 \times 10^3)\mathbf{g_1 g_2}/D(G)]^{1/3} \qquad (2)$$

Thus, the EPR data indicate that the radical and Co^{2+} are separated by ~11 Å in the active site.

In the recently reported crystal structure of the DDH complex with cyanocobalamin and 1,2-propanediol, C1 and

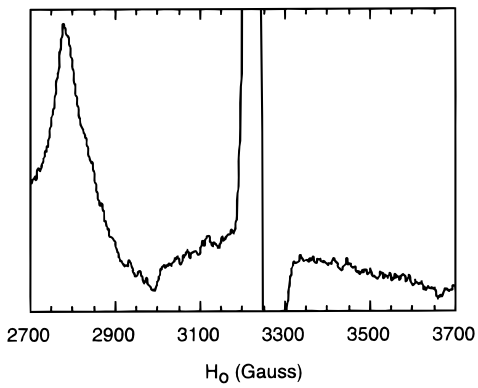

FIGURE 5: X-band EPR spectrum of a sample of EAL-coenzyme B_{12} following incubation for 1 min with glycoaldehyde. Components of the sample are given under Experimental Procedures. The spectrum was obtained at 77 K at a microwave frequency of 9.09 GHz and BMW microwave power.

C2 of propanediol are 8.4 and 9 Å, respectively, from the Co of the cyanocobalamin in the active site (*13*). The crystal structure also shows that hydroxyls of propanediol chelate to an essential K^+ in the active site. In the complex of the ethanesemidione, however, a proton occupies the position analogous to that of the K^+ in the complex with the substrate. Semidione anion radicals are known to chelate alkali metal ions in organic solvents such as DMSO (*20*). The present findings indicate that a proton is bound with high affinity to the *cis*-semidione, presumably in lieu of the K^+ that normally coordinates to the substrate. The switch from K^+ to a proton might account for the slightly longer distance between Co^{2+} and the backbone of ethanesemidione.

Interaction of Glycolaldehyde with EAL. DDH and EAL catalyze analogous coenzyme B_{12}-dependent, radical-mediated transformations starting with abstraction of a H-atom from C1 of the respective substrates (*27*). Assays of EAL exposed to 10 mM glycolaldehyde for various times indicate that glycolaldehyde inactivates EAL with an apparent rate of ~0.4 min^{-1}. The EPR spectrum of a sample in which a mixture of EAL and coenzyme B_{12} undergo a brief (~1 min) exposure to glycolaldehyde reveals the presence of signals due to B_{12r} and an organic radical (Figure 5). EPR spectra of samples prepared with isotopically substituted glycolaldehydes (Figure 6B−D) indicate that spin density of the radical is on the carbon skeleton of the glycolaldehyde precursor. As with the radical observed in inactivation of DDH by glycolaldehyde, spectra of samples prepared from [1-^{13}C]glycolaldehyde or [2-^{13}C]glycolaldehyde are indistinguishable and exhibit a modest broadening of the pattern (Figure 6B,C). Moreover, the EPR spectrum narrows for the sample prepared from perdeuterio glycolaldehyde (Figure 6D). The responses of the EPR spectra to isotopic substitutions in the glycolaldehyde precursor are analogous to those observed for the radical produced from glycolaldehyde by DDH; however, the spectrum that emerges from the sample with perdeuterio glycolaldehyde differs from that observed for the analogous sample with DDH (compare Figure 2D,E and Figure 6D). Differences in the electron spin−spin interactions between Co^{2+} and the radical in the active sites of DDH and EAL account for the differences in the spectra of the radical. Simulation (Figure 6E) of the signal obtained with perdeuterated glycolaldehyde ($D = -22$ G and $J = -11$ G) reveals that the major difference in the two

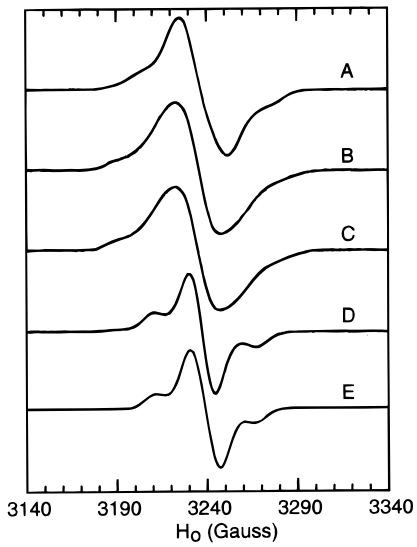

FIGURE 6: EPR spectra of the radical region of samples of EAL-coenzyme B_{12} after inactivation by glycoaldehyde. (A) Glycoaldehyde; (B) [C1-^{13}C]glycoaldehyde; (C) [C2-^{13}C]glycoaldehyde; (D) [$^2H_3$]glycoaldehyde; (E) simulation of the pattern in spectrum D with $D = -21$ G and $J = -11$ G. All samples were prepared in H_2O. Spectra were obtained at 1 mW microwave power at 77 K.

Scheme 3

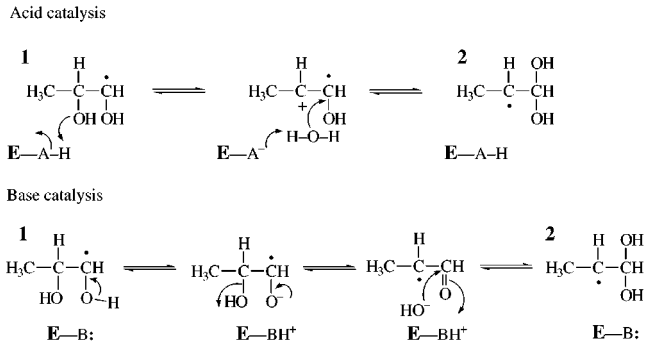

complexes is a larger ferromagnetic exchange interaction in the complex of EAL. The dipole−dipole interaction is approximately the same for the complexes of both enzymes, and this result indicates that the distance between the radical and Co^{2+} is virtually identical in the two enzymes. The source of the difference in the exchange interaction is presently unknown. At these relatively long distances the exchange interaction is mediated by intervening matter (superexchange) (*28*), and the difference in *J* between the two complexes could be due to slight differences in the positions of the matter separating the two paramagnetic species or in the orientation of the two paramagnetic species. Nevertheless, experiments with glycolaldehyde and EAL show that the ethanesemidione radical is the product formed upon H-atom abstraction from the semialdehyde as in the analogous reaction in the active site of DDH. This result reinforces the notion that the reactions catalyzed by these two enzymes share common steps and perhaps a similar overall architecture of active sites.

Mechanistic Implications. The mechanism by which 1,2-propanediol and other vicinal diols are rearranged to the corresponding aldehydes is still under investigation. The process is thought to be initiated by the abstraction of a hydrogen atom from C1 of the substrate by the 5′-deoxyadenosyl radical to produce substrate radical **1** in Scheme 2.

Scheme 4

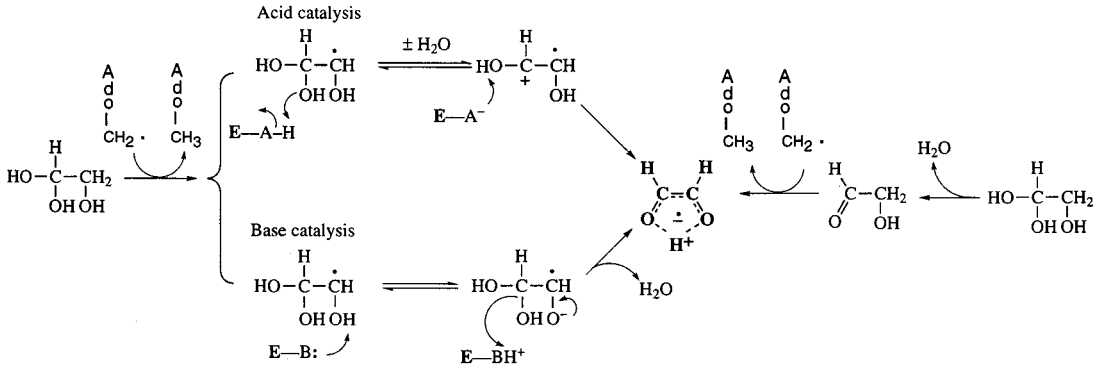

The possibilities for the further transformation of radical **1** into the radical precursor of hydrated propionaldehyde (radical **2** in Scheme 2) differ with respect to whether dehydration is brought about by acid or base catalysis, as illustrated in Scheme 3. If dehydration of radical **1** is by acid catalysis (*29*), a resonance-stabilized radical cationic intermediate is formed. The radical cation is then hydrated to the radical precursor of propionaldehyde hydrate (radical **2**). On the other hand, if base catalysis takes place (*30*, *31*), a ketyl radical is initially generated. The ketyl radical eliminates hydroxide to form a resonance-stabilized aldehyde radical. Addition of hydroxide to the aldehydic group generates the radical precursor to propionaldehyde hydrate. The acid/base groups in the active site that may participate in catalysis include His 143, Asp 335, and Glu 170 in the α-subunit (*13*).

Glycolaldehdye is extensively (i.e., >95%) hydrated in aqueous solution. If the predominant hydrated form binds in the active site and undergoes H-atom abstraction prior to dehydration, closely related mechanisms, illustrated in Scheme 4, can be written for the formation of the semidione radical in suicide inactivation by glycolaldehyde. After abstraction of a H-atom at the methylene group of the glycolaldehyde hydrate to form the analogue of radical **1**, elimination of water may take place by one of the pathways in the left half of Scheme 4. The planar cationic radical resulting from acid-catalyzed dehydration can lose a proton to form the semidione radical. In the base-catalyzed dehydration, the ketyl radical resulting from the initial proton abstraction can eliminate hydroxide to form the semidione radical. Alternatively, H-atom abstraction from the methylene of the aldehyde form of the inactivator leads directly to the semidione radical as shown in the right-hand side of Scheme 4. The hydrate of glycolaldehyde could use the resident dehydration machinery to convert to the aldehyde prior to H-atom abstraction. In each of these mechanisms, the highly delocalized semidione radical is easily formed from the glycolaldehyde analogue of a radical intermediate in the normal reaction mechanism. In any case, the formation of the semidione radical ends the reaction of glycolaldehyde, because a hydrogen atom is never reabstracted from 5′-deoxyadenosine. The highly delocalized semidione radical does not possess sufficient oxidizing capacity to recapture a H-atom from 5′-deoxyadenosine. The resistance of the semidione radical toward reduction also prevents this "alien" radical from damaging the active site through oxidation of an amino acid side chain. Thus, the semidione radical represents a free energy "hole" relative to the 5′-deoxyadenosyl radical that would be generated in the next step of the reaction of a true substrate. The complex of DDH, B_{12r}, and the *cis*-ethanesemidione radical is stable under anaerobic conditions for several days, and the active site is blocked from further reactions. Under aerobic conditions, one-electron oxidation of the radical by triplet oxygen gives glyoxal, but the high affinity of the enzyme for B_{12r} prevents the entry of fresh coenzyme B_{12} for further cycles of oxidation (*14*). Semidione radical formation by any of the mechanisms in Scheme 4 is entirely consistent with the fact that the inactivation of DDH by [2-^{3}H]glycolaldehyde leads to the incorporation of tritium into the 5′-deoxyadenosine formed from the cleavage of adenosylcobalamin (*32*). Similar arguments apply to the transformation of glycolaldehyde to the ethanesemidione radical in the active site of EAL. Inactivation of DDH and of EAL by glycolaldehyde is analogous to the inactivation of EAL by hydroxyethylhydrazine (*18*) in the sense that glycolaldehyde and hydroxyethylhydrazine are converted into stable radicals that do not have the oxidizing capacity to abstract H-atoms and complete the catalytic cycle.

ACKNOWLEDGMENT

We thank Dr. Thomas A. Bobik for supplying a plasmid containing the genes encoding the subunits of DDH, and Dr. Bernard Babior and Ms. La Rosa Faust for plasmid pKQE4.5 containing the genes for EAL.

REFERENCES

1. Lee, H. A., and Abeles, R. H. (1963) *J. Biol. Chem. 238*, 2367−2373.
2. Frey, P. A. (1990) *Chem. Rev. 90*, 1343−1357.
3. Frey, P. A. (1997) *Curr. Opin. Chem. Biol. 1*, 347−356.
4. Lawrence, C. C., and Stubbe, J. (1998) *Curr. Opin. Chem. Biol. 2*, 650−655.
5. Halpern, J., Kim, S.-H., and Leung, T. W. (1984) *J. Am. Chem. Soc. 106*, 8317−8319.
6. Finke, R. J., and Hay, B. P. (1984) *Inorg. Chem. 23*, 3041−3043.
7. Licht, S., Gerfen, G. J., and Stubbe, J. (1996) *Science 271*, 477−481.
8. Hogenkamp, H. P. C. (1999) in *Chemistry and Biochemistry of B12* (Banerjee, R., Ed.) pp 3−8, Wiley-Interscience, New York.
9. Retey, J., Umani-Ronchi, A., Sebl, J., and Arigoni, D. (1966) *Experientia 22*, 502−503.
10. Zagalak, B., Frey, P. A., Karabatsos, G. L., and Abeles, R. H. (1966) *J. Biol. Chem. 241*, 3028−3035.
11. Schepler, K. L., Dunham, W. R., Sands, R. H., Fee, J. A., and Abeles, R. H. (1975) *Biochim. Biophys. Acta 397*, 510−518.

12. Toraya, T., Krodel, E., Mildvan, A. S., and Abeles, R. H. (1979) *Biochemistry 18*, 417−426.
13. Shibata, N., Masuda, J., Tobimatsu, T., Toraya, T., Suto, K., Morimoto, Y., and Yasuoka, N. (1999) *Structure 7*, 997−1008.
14. Wagner, O. W., Lee, H. A. J., Frey, P. A., and Abeles, R. H. (1966) *J. Biol. Chem. 249*, 1751−1762.
15. Fontecave, M., and Mulliez, E. (1999) in *Chemistry and Biochemistry of B12* (Banerjee, R., Ed.) pp 731−756, Wiley-Interscience, New York.
16. Abend, A., Bandarian, V., Nitsche, R., Stupperich, E., and Retey, J. (1998) *Angew. Chem., Int. Ed. Engl. 37*, 625−627.
17. Faust, L. P., Connor, J. A., Roof, D. M., Hoch, J. A., and Babior, B. M. (1990) *J. Biol. Chem. 265*, 12462−12466.
18. Bandarian, V., and Reed, G. H. (1999) *Biochemistry 38*, 12394−12402.
19. Morton, J. R. (1964) *Chem. Rev. 64*, 453−471.
20. Russell, G. A. (1968) in *Radical Ions* (Kaiser, E. T., and Kevan, L., Eds.) pp 87−150, Wiley-Interscience, New York.
21. Pake, G. E. (1948) *J. Chem. Phys. 16*, 327−336.
22. Abragam, A., and Bleaney, B. (1970) *Electron Paramagnetic Resonance of Transition Ions*, Oxford Univeristy Press, Oxford, England.
23. Eaton, G. R., and Eaton, S. S. (1989) *Biol. Magn. Reson. 8*, 339−397.
24. Eggerer, H., Stadtman, E. R., Overath, P., and Lynen, F. (1960) *Biochem. Z. 333*, 1−9.
25. Gerfen, G. J. (1999) in *Chemistry and Biochemistry of B12* (Banerjee, R., Ed.) pp 165−195, Wiley-Interscience, New York.
26. Luckhurst, G. R. (1976) in *Spin Labeling: Theory and Practice* (Berliner, L. J., Ed.) pp 133−181, Academic Press, New York.
27. Toraya, T. (1999) in *Chemistry and Biochemistry of B12* (Banerjee, R., Ed.) pp 783−809, Wiley-Interscience, New York.
28. Owen, J., and Harris, E. A. (1972) in *Electron Paramagnetic Resonance* (Geschwind, S., Ed.) pp 427−492, Plenum, New York.
29. Walling, C., and Johnson, R. A. (1975) *J. Am. Chem. Soc. 97*, 2405−2407.
30. Bansal, K. M., Gratzel, M., Henglein, A., and Janata, E. (1973) *J. Phys. Chem. 77*, 16−19.
31. Lenz, R., and Giese, B. (1997) *J. Am. Chem. Soc. 119*, 2784−2794.
32. Frey, P. A. (1968) Ph.D. Thesis, Brandeis University.

BI992963K